Seismic Performance of Underground Pipes during the Canterbury Earthquake Sequence

A.K. Sherson

Student, University of Waikato, Hamilton, New Zealand

M. Nayyerloo & N.A. Horspool

GNS Science, Lower Hutt, New Zealand

ABSTRACT: The recent Canterbury Earthquake Sequence revealed new information about how underground water pipes behave during an earthquake, especially under the influence of liquefaction. Due to the vast amount of data that the Canterbury sequence provided, new Modified Mercalli Intensity -based fragility curves were able to be produced. This paper presents the results from studies on how the water, wastewater and storm water networks in Christchurch performed during the Canterbury earthquake sequence. Difficulties that arose from the complex sequence of earthquakes will be discussed, focusing on the way the pipes behaved during the February and June 2011 aftershocks and contrasting the effects that the two earthquakes had on the city, how the network behaved during each event, as well as discussing the effects of multiple earthquakes. A brief look into how the network was repaired over time will also be discussed, including differences between pipe networks and their repair priorities. Finally, methodologies of deriving Modified Mercalli Intensity and liquefaction maps and their effect on the derived fragility cures will be discussed, touching on the shortcomings of instrumental Modified Mercalli Intensity and drive-by surface observations in liquefaction analyses.

1 INTRODUCTION

The Canterbury 2010-2011 Earthquake Sequence (CES) was very damaging to underground water pipes in Christchurch, causing widespread interruptions in service, for many months. Hundreds of thousands of residents were effectively cut off from the water supply, storm water and wastewater networks as a result of the earthquakes, and many systems were classified as being on the brink of failure (Eideinger, et al., 2012). To combat the shortages, and to reduce the health impacts to the community, hundreds of temporary fresh water tanks and pumps were distributed around the city, along with 10,000 portaloos and 30,000 chemical toilets. For two weeks following the February Earthquake a boil water restriction was imposed, due to concerns about contamination of the fresh water sources, and the risk of breakouts of disease and sickness. Widespread damage to the wastewater network and waste treatment plant lead to 60 million litres of untreated wastewater being discharged straight into multiple local water bodies and streams, with the risk of contaminating the underground aquifers (Eideinger, et al., 2012). From October 2010 to February 2014, 8,556 repairs were commissioned to be completed on the water supply network, and 1,726 repairs on the wastewater network. The storm water network is still under repair, and currently 21,692 faults have been discovered on the network, of which 20,482 need repair or some "action".

The storm and waste water repairs are classified differently to the water supply repairs which are based off contractors' repair notes. Contractors' notes often group multiple faults in one location, and record the group as one fault, unlike the CCTV repair process, used to investigate storm and waste water pipes which classifies repairs as separate faults. Additionally, not all repairs to the network were economically viable, as some repairs would not be able to increase the functionality of the pipe enough to cover the cost of repair (SCIRT, 2013). Moreover, in the aftermath of the CES, the focus was on restoration of service rather than improving the resilience. Therefore, repairs had to be

prioritised.

This paper presents the results from studies on how the water, wastewater and stormwater networks in Christchurch performed during the Canterbury earthquake sequence (CES), focusing on the two most damaging aftershocks of February and June 2011. The performance has been studied for the main pipe material types present in the three networks, and is described through fragility models which are functions of both shaking intensity and ground conditions. Brief information on the events and the three networks affected are provided in the following sections, followed by a description of the data and methodologies used to derive the fragility models. Finally, the results are presented, and the shortcomings of instrumental intensities and drive-by surface observations of liquefaction are discussed, focusing on the effects on the models developed.

2 CANTERBURY EARTHQUAKE SEQUENCE

On 22nd February, 2011, Christchurch City experienced a direct hit from a destructive magnitude (Mw) 6.2 aftershock following the main event of magnitude 7.1 on the 4th September, 2010. The February event was followed by another destructive aftershock of magnitude 6.4 in June and later by a magnitude 6.0 aftershock in December. There were also numerous aftershocks of smaller magnitudes in between and after these main events. The February and June events caused severe shaking and widespread liquefaction in Christchurch, which caused significant damage to Christchurch's underground water pipes. Liquefaction caused ingress of sediments to the pipes, failure of pipes due to uneven settlement, uplift of unpressurised pipes, pull-outs of joints etc. The liquefaction was widespread but most severe in the suburb of Bexley and along the Avon River (Cubrinovski, Hughes, & O'Rourke, 2013).

2.1 *Shaking intensity*

The shaking intensities in Modified Mercalli Intesity (MMI), for both the February and June events were estimated using 'ShakeMapNZ', which is the modified version of the US ShakeMap for New Zealand. For estimating intensities, ShakeMapNZ uses the model of Allen et al. (2012) which includes macro-seismic intensity data from around the globe as well as from over 100 New Zealand events. For the February and June events, the inter-event uncertainty in the intensity prediction equation was removed by converting all observed instrumental ground motions on 25 GeoNet (www.geonet.org.nz) strong motion recording stations around Christchurch, into macro-seismic intensity using the Ground Motion to Intensity Conversion Equation (GMICE) of Worden et al (2012). More details of the methods used in ShakeMapNZ can be found in Horspool et al. (2015).
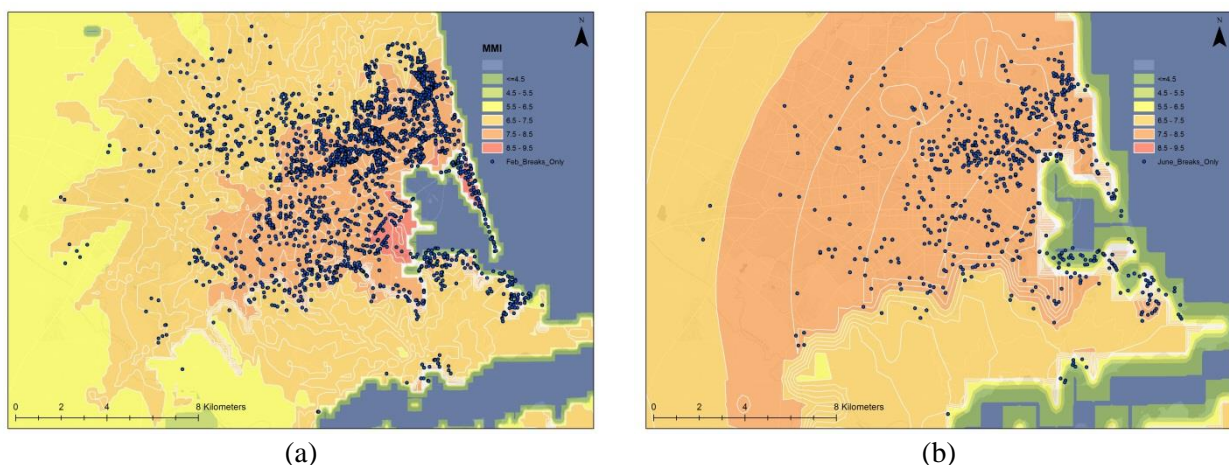

| (a) | (b) |

Figure 1. MMI maps from a) the 22nd February 2011 and b) the 13th June 2011 earthquakes. MMI5, for example, is the range between MM4.5 and 5.5 and so forth. The dots represent breaks to the water supply network.

2.2 *Liquefaction*

Extensive liquefaction is believed to be the main cause of substantial damage to Christchurch buried water pipes, although it is still unclear how much of the so called 'liquefaction' was actually due to increase in the confined artesian water pressure and flooding through cracks in the aquiclude (Cox, 2015). One example of liquefaction damage was the uplift or floating of unpressurised pipes, such as storm water and wastewater pipes, which lead to the direction of invert changing, causing fluids to flow in undesirable directions. Rapid uplift of the pipes also caused pull-outs and shearing of joints in both pressurised and unpressurised pipes (Eideinger, et al., 2012).

The liquefaction severity maps used in this study were produced by Tonkin and Taylor Ltd. using information collected from drive-through surveys, where evidence from liquefaction was mapped, taking into account visible lateral spreading, sand boil deposits, and land damage etc. (Canterbury Geotechnical Database, 2013) (Fig. 2). Liquefaction was divided into 6 classes depending on the severity of the manifestation:

- Class 0: Not observed, presumed no liquefaction
- Class 1: No observed damage
- Class 2: Minor land damage but no observed liquefaction
- Class 3: Moderate liquefaction but no lateral spreading
- Class 4: Severe liquefaction but no lateral spreading
- Class 5: Moderate to major lateral spreading
- Class 6: Severe lateral spreading

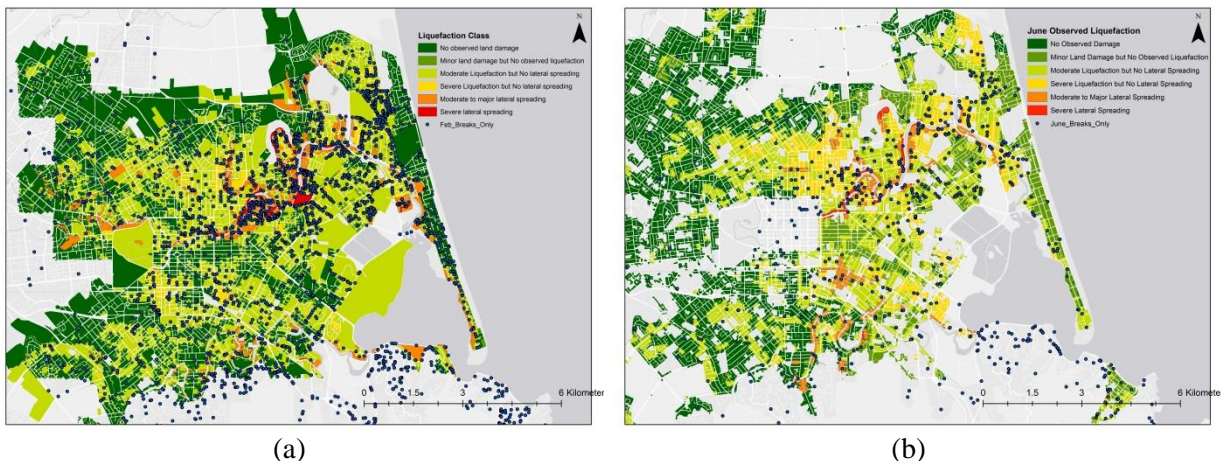| (a) | (b) |

Figure 2. Observed liquefaction maps from Tonkin and Taylor for a) the February event, and b) the June event. The dots represent breaks to the water supply network.

In this paper the extent of liquefaction, and its implications when producing a fragility curve, will be discussed along with its effects on the overall break rates in Christchurch. The hampered repair process will also be discussed, aiming to understand what occurred in Christchurch and the lessons we can gain from studying the performance of the Christchurch underground pipes during the CES.

3 OVERVIEW OF NETWORK

3.1 *Water Supply*

Christchurch City's water supply network is made up of similar lengths of mains and sub-mains, each about 1,700km long. The mains consist of mainly brittle materials such as Asbestos Cement (AC, 50%) and Cast Iron (CI, 12%). The mains also contain some ductile materials such as, Polyvinyl Chloride (PVC, 12%), Medium-density PVC (MPVC, 8%) and Un-plasticised PVC (UPVC, 6%). The

other 12% is a mixture of 16 ductile and brittle materials. Conversely, the submains consist of mainly ductile materials such as Polyethylene (PE, 52%), Medium-density PE (MDPE80, 26%), and Galvanised Iron (GI, 12%). The other 10% is made of a mixture of 14 ductile and brittle materials. All of the Christchurch water is obtained from underground aquifers pumped from approximately 150 wells at 50 different sites, and then stored in 8 main reservoirs and another 37 service reservoirs (Cubrinovski et al., 2011). This network provides 100,000 cubic meters a day (100 million litres a day), totalling to about 36,525,000 cubic meters a year (36.5 Billion litres a year) (Eideinger & Tang, 2012).

3.2 *Wastewater*

The Christchurch wastewater network comprises around 2,000km of wastewater pipes. 70% of the pipes are made of brittle materials such as Concrete (CON), AC, and Earthenware (EW). The network services the entire population of Christchurch city, and has a capacity of around 6,000 litres per second, (518 million litres a day) (Christhchurch City Council, 2013).

3.3 *Storm Water*

The storm water network collects all rainwater and runoff from Christchurch and discharges it into local rivers and streams, through 2,000km of underground pipes. The pipes are mostly made of brittle materials, Reinforced Concrete (RC, 54%), CON (5%), EW (5%) and AC (8%), covering about 70% of the network. The other 30% is constructed from various other materials, which are mostly ductile.

4 METHODOLOGY

The water supply, waste water and storm water network information including the material type, age, diameter, length and location was supplied by Christchurch City Council (CCC), Stronger Christchurch Infrastructure Rebuild Team (SCIRT) and City Care Ltd. The pipes were then segmented into 20-metre or shorter segments. This was done to ensure that each segment obtains the characteristics of the soil that it is laid in when the segment centroid is used to represent the pipe location. Each segment was then assigned a shaking intensity in MMI by geospatially joining the pipe centroid locations with the event MMI maps. Observed liquefaction severity categories were also assigned in a similar way by spatially joining the centroid locations with the observed liquefaction severity maps from Tonkin and Taylor.

4.1 *Damage Data*

Pipe repair data were supplied by City Care Ltd for each of the three waters independently. Damage to water supply pipes was found primarily from surface observations and pressure changes. For storm and waste water pipes, CCTV inspections were used, noting all the faults to the pipe, from pipe cracks to large pipe pull outs (SCIRT, 2013). Pipe repairs were recorded by various contractors, where the repair notes included limited information about the type of repair, repair date, and length of pipe repaired. Unfortunately, a lot of these data were incomplete, and different contractors used different terminologies in the repair processes. Therefore, there was no complete database containing accurate, comprehensive repair or replacement information. Many contractors only recorded the minimum amount of information such as "AC pipe replaced", or "3m pipe repaired", without detailing the repair process or the material used to replace the pipe. However, considering that documenting the damage was not the contractors' highest priority in the aftermath of the CES, invaluable data was recorded, which will be useful to better understand the seismic performance of buried water pipes.

Inspection dates (or repair request dates) were all recorded correctly. Thus this information was used to understand which event caused what damage. However, the sequence of damaging aftershocks made it difficult to understand what damage was caused by which event to enable the correlation between the damage and the associated shaking intensities and observed liquefaction for each event. For example, it is not clear whether all the damage caused by a particular event in the sequence was

found before the next event or how much of the damage recorded was pre-existing before the main shock of September 2010. For water and wastewater networks, which were repaired after each event as much as practical, the recorded inspection dates (or repair request dates) were helpful to differentiate the damage caused by each of the main events in the CES although some assumptions had to be made.

To calculate the time taken to restore the network after each event, or the period within which all reported damage could be associated with the event and was not pre-existing damage or damage caused by the previous event in the sequence, O'Rourke, et al., (2014) suggest that as the network is restored, the cumulative rate of repair (repairs per day), follows a pattern of initial high rate of repair, followed by a transient state with an intermediate repair rate and finally a steady state of repair with a rate close to the pre-earthquake rate of repairs (business as usual) (Fig 3). The beginning of the steady state of repair shows where the repair period associated with the event ends.

Such tri-linear trends could only be established for the water network. For the February earthquake this steady state of repair occurs around April 15th 2011. Therefore, all repairs identified in the inspection process before April 15th, were considered faults/breaks directly related to the February earthquake. For the June event, the onset of transition to the steady state was almost two months from the event in mid-August. For the wastewater network in the absence of clear transition points, an averaging technique was used, which will be discussed in the following section. For storm water pipes, the repairs were delayed by months until after the June event. Therefore, it was not possible to correlate the damage with any of the events to derive suitable fragility models.

Each repair was then geospatially joined with the pipe network data for each network type, for both February and June earthquakes. The break rates or repair rates for each pipe class (combination of material type and size) and shaking intensity bin were then calculated by dividing the number of repairs over the total length of pipes within the class and the intensity bin.

4.2 *Averaging of Wastewater break rates*

All breaks reported after the February earthquake and before the June event were assumed to be related to the February event, and the repairs after the June earthquake up to the steady state of repair, 10th of November 2011, were assumed to be associated with the June earthquake. The relevant shaking intensity and liquefaction maps were then used for each event separately to put the breaks into different shaking intensity and liquefaction severity bins for each pipe class. The average break rate for each combination of intensity and liquefaction severity was then calculated for each pipe class by adding the total number of breaks from each event and dividing the sum by the total length of pipes of the same class affected in each event. This is superior to the method used in O'Rourke et al. (2014) that averages the break rates of the two events, and yields a weighted average based on the total length of pipe affected in each event.

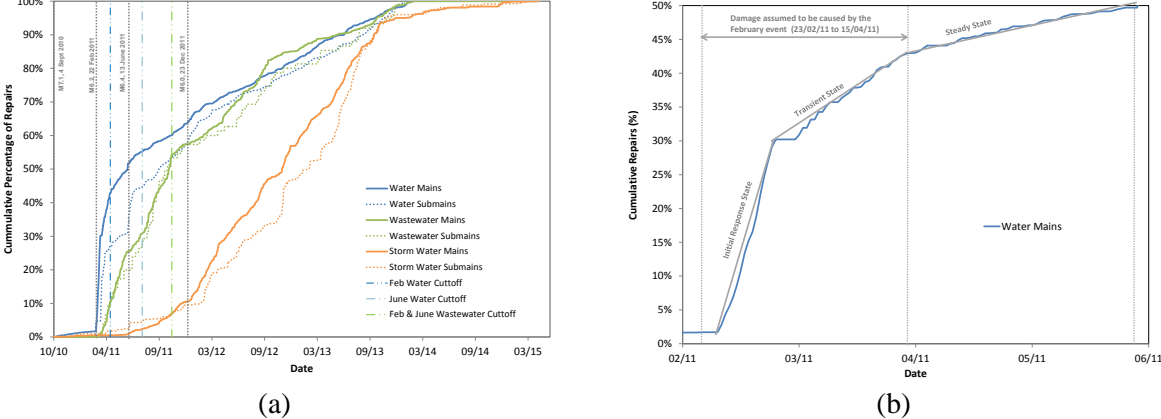(a)   (b)

Figure 3. Cumulative repairs to the network, showing the process of how each system was repaired. (a) Displays the entire repair process from October 2010 to May 2015, (b) shows the repair process from February 2011 to June 2011 for the water mains only.

5

4.3 *Damage Data Screening*

Each data point (pipe class repair rate) was then put through a screening process, to remove extreme values that arose from low sample sizes (i.e. pipe lengths). The screening criterion used is similar to the one proposed by O'Rourke and Deyoe (2004) and ensures the repair rates are within 50% of the 'true' repair rates with 95% confidence. The use of this screening criterion removed all break rates that were based on a total length less than the minimum length specified by the criteria for the break rate to be within 50% of the true rate with 95% confidence.

5 RESULTS AND DISCUSSION

5.1 *Results*

Overall break rates for the entire city are reported in Tables 1 and 2 by material type for water and wastewater networks, independently. More detailed break rates for each pipe class and different combinations of intensity and liquefaction severity are shown in Figure 4. As Table 1 shows, overall, the June break rates were lower than the February break rates. This is, broadly speaking, consistent with the lower amount of liquefaction manifestation (Eideinger et al., 2012) and shaking experienced in the June event. The June break rates might also be affected by the fact that many weak points in the network were already damaged in the February event and most were repaired in the two months following the event, resulting in a slightly enhanced seismic resilience in the network. However these repairs or replacements between events are not expected to have a large effect on the total lengths reported for each material type in the table, as around less than 1% of the network was replaced with more resilient material. The results also show that pipes made of ductile material such as HDPE, MDPE and PVC performed a great deal better than those made of brittle material such as AC, CI. Small galvanised Iron pipes were the worst performing class among the different pipe classes present in the Christchurch three waters networks. GI pipes are used mainly as laterals and therefore are very small (usually 20 or 25 mm in diameter) and have many connections. The galvanised pipes are also all laid before 1980 and in some cases are around 100 years old and possibly a lot of them are now corroded. Combination of these factors is deemed to have contributed to the very high break rates for this class of pipe. Lastly, the ratios of break rates in liquefied areas (affected by permanent ground motions) over the break rates in non-liquefied areas (affected by transient ground motions) for the pipe materials studied ranges from 2 to 10 and supports the suggestion that pipes are more vulnerable to permanent ground motions than to transient motions. Similar results can be drawn from the wastewater repair rates. However, these results ignore variations in the pipe sizes and shaking intensities affecting pipes within each material class.

Figure 4 shows the break rate results in more detail for Christchurch water and waste water networks and both of the February and June events. Each point on the graph represents how a particular class of pipe (combination of material type and size) performed during the February or June event when subjected to a particular level of shaking and was in a particular ground condition (liquefied or non-liquefied). This way the effects of all contributing factors to damage are captured. Figure 4 confirms the previous conclusions drawn from the tabulated break rates. It also shows an increasing trend in the break rates with shaking intensity although for some pipe classes this may not be evident due to lack of data. As can be seen in the figure, there are no instances where different sizes of pipe, of the same material and in the same class of ground, were exposed to the same level of shaking, and so it was not possible for the effect of size on the seismic performance of pipes to be evaluated. However, larger pipes usually tend to be more robust to seismic loading compared to smaller pipes.

5.2 *Combination with Global Damage Data*

Reports of damage to water supply pipelines in eleven major earthquakes as well as three major reviews of the topic (ALA 2001, 2005, Rojahn and Sharpe 1985) have been reviewed by Cousins (2013). A great deal of descriptive information was found with incomplete and often inconsistent data with high variability. However, Cousins observed these general trends within the available data, which

are all consistent with the Christchurch observations: (a) damage increases with shaking intensity, (b) increases greatly when ground damage (liquefaction or lateral spreading) occurs, (c) decreases with increasing pipe diameter, and (d) depends on pipe material and jointing method.

The data that Cousins used were screened according to the criteria explained in 4.3 above (shown as grey points in Figure 4) and combined with the Christchurch data to derive appropriate fragility models. Some of the data were lost during the screening because there was not enough surveyed length information to establish whether the minimum sample size requirement was met. The effect of size was also had to be ignored to enable the combination and therefore the reported fragility models for each class are applicable to all pipes smaller than 300 mm. The power model of Equation 1 best fitted the data for most classes with a very few exceptions. However, in those cases the coefficient of determination (R^2) was too low (<0.25) for the respective trendline to be reported:

$$BR \ [km^{-1}] = a \times MMI^{\ b} \qquad \qquad \text{(Equation 1)}$$

Here, BR is the break rate in breaks per kilometre and 'a' and 'b' are curve fitting constants for the pipe class as shown in Table 3. As can be seen in the table, the R-squared values are quite low for some classes, which show that variations in the break rates for some classes are not adequately captured by varying intensity. Therefore, the reported vulnerability models should be used with caution.

Table 1. Break rates for water pipes in the February and June earthquakes

	Pipe Material	Pipe Length (km)	Length %	No. of Breaks	Overall Average Break Rate	Breaks in Liquefied Areas	Breaks in Non Liquefied Areas	Pipeline length in Liquefied Areas (km)	length in non Liq Areas (km)	Ave. Break Rate in Liq. Areas	Ave. Break Rate in Non Liq. Areas	Ratio (Liq/Non-Liq)
Feb.	HDPE	923.2	26.4%	456	0.5	286	170	337.3	585.9	0.8	0.3	2.9
	AC	902.9	25.8%	1022	1.1	732	290	236.0	666.9	3.1	0.4	7.1
	MDPE 80	461.8	13.2%	98	0.2	71	27	132.8	328.9	0.5	0.1	6.5
	PVC	272.4	7.8%	78	0.3	56	22	80.9	191.5	0.7	0.1	6.0
	CI	227.1	6.5%	252	1.1	191	61	98.0	129.1	1.9	0.5	4.1
	GI	212.0	6.1%	962	4.5	649	313	88.5	123.6	7.3	2.5	2.9
	Other	499.8	14.3%	154	0.3	119	35	135.3	364.5	0.9	0.1	8.5
	TOTAL	3,499.3		3,022		2,104	918	1,108.8	2,390.4			
June	HDPE	923.3	26.7%	126	0.1	70	56	329.9	593.4	0.2	0.1	2.2
	AC	901.8	26.1%	248	0.3	162	86	223.8	678.1	0.7	0.1	5.7
	MDPE 80	465.2	13.5%	21	0.0	13	8	144.7	320.5	0.1	0.02	3.6
	PVC	271.5	7.9%	20	0.1	15	5	78.6	192.9	0.2	0.03	7.4
	CI	225.9	6.5%	71	0.3	37	34	86.2	139.6	0.4	0.2	1.8
	GI	211.9	6.1%	201	0.9	139	62	78.9	133.0	1.8	0.5	3.8
	Other	454.9	13.2%	52	0.1	41	11	121.1	333.7	0.3	0.03	10.3
	TOTAL	3,454.5		739		477	262	1,063.2	2,391.3			

Table 2. Wastewater pipes break rates for the combined and averaged data (Both February and June)

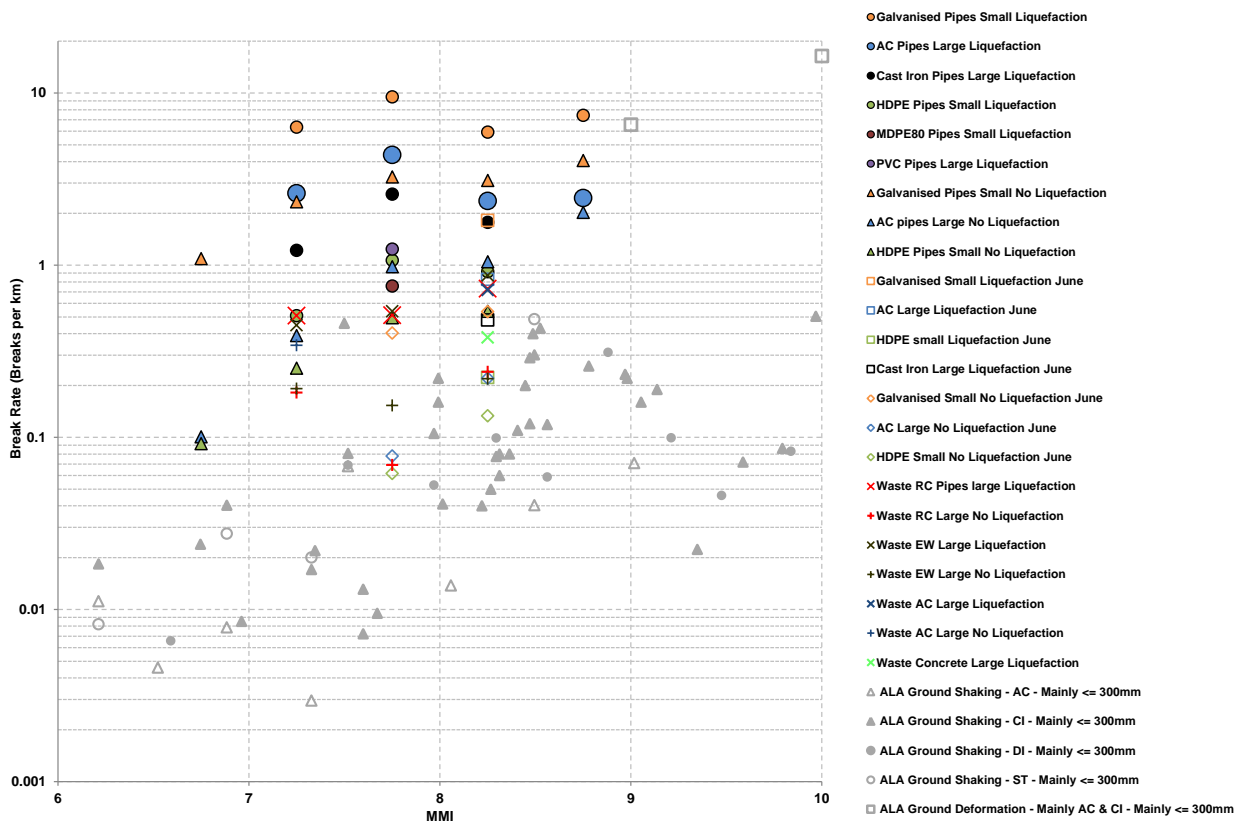| Pipe Material	Combined Pipe Length (km)	Combined Length %	Combined No of Breaks	Overall Average Break rate	Breaks in Liquefied Areas	Breaks in Non Liq-uefied Areas	Pipeline Length in Liquefied Areas (km)	Length in Non Liq Areas (km)	Ave Break Rate in Liq Areas	Ave Break Rate In Non Liq Areas	Ratio Liq/Non-Liq
RCRR	1,366.6	0.3	356	0.26	255	101	408.3	958.3	0.62	0.11	5.9
EW	783.8	0.2	345	0.44	255	90	342.6	441.1	0.74	0.20	3.6
UPVC	722.6	0.2	39	0.05	25	14	118.9	603.7	0.21	0.02	9.1
AC	370.6	0.1	81	0.22	50	31	92.0	278.6	0.54	0.11	4.9
CONC	281.8	0.1	64	0.23	48	16	146.8	134.9	0.33	0.12	2.8
PVC	104.7	0.0	5	0.05	1	4	18.9	85.8	0.05	0.05	1.1
CI	60.1	0.0	19	0.32	14	5	29.5	30.6	0.47	0.16	2.9
HDPE	46.4	0.0	10	0.22	7	3	12.3	34.1	0.57	0.09	6.5
Other	297.0	0.1	6	0.02	5.0	1.0	96.9	200.2	0.05	0.00	10.3
Total	4,033		925		660	265	1,266	2767			

Figure 4. Christchurch water and waste water pipes break rates for different combinations of pipe material and size, calculated for different shaking intensity levels and ground liquefaction susceptibilities. Small wastewater pipes are smaller than 150mm and small water supply pipes are smaller than 100mm.

Table 3. Parameters of the fragility models derived

Pipe Material	Ground Condition	a	b	R^2
AC	Non-liquefied	5.00E-10	9.3236	0.2466
	Liquefied	1.00E-05	5.8428	0.3027
CI	Non-liquefied	8.00E-08	6.5747	0.3255
	Liquefied	5.00E-08	8.3512	0.5703
RC	Liquefied	2.00E-03	2.7591	0.7421
EW	Liquefied	2.00E-05	5.1093	0.9297
DI	Non-liquefied	6.00E-07	5.4013	0.4407
ST	Non-liquefied	6.00E-13	12.659	0.8807

5.3 *Discussion*

The effect of liquefaction in Christchurch was both horizontally and vertically non uniform, with large changes in severity even inside the same liquefaction severity class (Cubrinovski, Hughes & O'Rourke, 2013). Not only did the underground reticulation network experience high changes in liquefaction observable at the surface, it experienced additional subsurface liquefaction at higher severities and variability, than the liquefaction map suggests (Cubrinovski, Hughes, & O'Rourke, 2013) (O'Rourke, et al., 2014). This sporadic nature of liquefaction had a large influence on the overall break rates. For example, GI pipes in the severe liquefaction region had break rates of up to 8 breaks per km, which is close to 20 times higher than the break rates observed in similar sized GI pipes subjected to the same level of shaking but in non-liquefied areas.

Huge uncertainties in the estimated ground motion intensities used to correlate damage to ground shaking intensity also had a large influence on the results. There is up to 1 full MMI unit uncertainty in the estimated intensities. Therefore, the cloud of break rate data points in Figure 4 could be shifted one MMI unit to the left or right horizontally. However, comparing the ShakeMapNZ predicted intensities for the February earthquake with same results based on GeoNet 'Felt Reports' submitted by the public combined with data on observed damage to buildings shows that the ShakeMap intensities are on average about one MMI unit lower for the MMI range above 8.0 and therefore underestimate the higher shaking intensities (Goded, et al., 2014 and Stirling, et al., 2015). This is consistant with the amount of liquefaction damage observed in Christchurch in the February event. For example the highest break rates in Christchurch occurred in the eastern suburbs, directly related to the severity of liquefaction, around an MMI of close to 8.0, while the highest shaking intensities occurred further south, governed by average break rates in Figure 4.

The influence of multiple large earthquakes/aftershocks also raises more questions on how much of the damage considered to be caused by an event was actually caused by that event and was not pre-existing as a result of a previously occurred event. Further study is therefore required to better understand how the buried services in Christchurch performed during the CES and whether the Christchurch results could be directly applicable to other areas for modelling risk to underground pipes from earthquakes.

6 CONCLUSION

This paper combined the invaluable damage data that the Canterbury Earthquake Sequence provided, with the existing damage data globally, and proposed better informed Modified Mercalli Intensity (MMI)-based fragility curves for modelling damage to buried water pipes in earthquakes, especially under the influence of liquefaction. The fragility models proposed are based on damage data that were screened systematically to ensure the true performance of pipes is captured and in that sense is superior to the existing models. As with most empirical fragility models, the proposed models are not well-supported by data, and since they are based on the Modified Mercalli Intensity, inherit the subjective-ness of the macro-seismic scale. Work is currently underway to develop fragility models which are based on engineering demand parameters to address this issue.

7 ACKNOWLEDGEMENT

REFERENCES:

ALA (2001). American Lifelines Alliance, Seismic fragility formulations for water systems, Part 1 – Guideline, Part 2 – Appendices. *ASCE.* http://www.americanlifelinesalliance.org/

ALA (2005). American Lifelines Alliance, Seismic guidelines for water pipelines, *ASCE*, March 2005. http://www.americanlifelinesalliance.org/

Allen, T.A., Wald, D.J. & Worden, C.B. (2012) Intensity attenuation for active crustal regions, *Journal of Seismology*, 16:409–433. DOI 10.1007/s10950-012-9278-7

Canterbury Geotechnical Database (2013) "Liquefaction and Lateral Spreading Observations", *Map Layer CGD0300,* Retrieved 4 July 2015 from https://canterburygeotechnicaldatabase.projectorbit.com

Christchurch City Council (2013) *Christchurch City Council website,* Wastewater Facts and Figures, http://www.ccc.govt.nz/homeliving/wastewater/wastewatercollection/factsandfigures.aspx , Retrieved 5 May 2015.

Cousins, W.J. (2013) Wellington Without Water – Impacts of Large Earthquakes, *GNS Science Report 2012/30,* 124 p.

Cox, S. (2015). Did Artesian Water Have an Effect on the Liquefaction Damage in Christchurch? , *New Zealand Natural Hazards Research Platform Presentation Series*, 23 February 2015, GNS Science, Wellington.

Cubrinovski, M., Hughes, M., & O'Rourke, T. D. (2013) Impacts of Liquefaction on the potable water system of Christchurch in the 2010-2011 Canterbury (NZ) earthquakes. *Journal of Water Supply: Research and Technology-Aqua*, 63(2):95-105.

Cubrinovski, M., Hughes, M., Bradley, B., McCahon, I., McDonald, Y., Simpson, H., et al. (2011) Liquefaction Impacts on Pipe Networks, *NZ Natural Hazards Research Platform Short Term Recovery Project No. 6*, University of Canterbury, available at http://ir.canterbury.ac.nz/handle/10092/10178 (Access Date: 30 June 2015).

Eideinger, P., Tang, A., O'Rourke, T., Baska, D., Davis, C., Kwasinski, A., et al. (2012) Christchurch New Zealand Earthquake Sequence of Mw 7.1 September 04, 2010 Mw 6.3 February 22, 2011 Mw 6.0 June 13,

2011: Lifeline Performance. *Technical Council on Lifeline Earthquake Engineering Monograph No. 40 February 2012 – Revision 0.*

Goded, T., Ingham, J.M., Giovinazzi, S., Lagomarsino, S., Clark, W., Cattari, S., Ottonelli, D., Marotta, A., Lourenço, P.B. & McClean R. (2014) Vulnerability analysis of unreinforced masonry churches, *EQC biennial Contestable Round Project 14/660* (Unpublished Preliminary Report).

Horspool, N.A., Chadwick, M., Ristau, J., Salichon, J. & Gerstenberger, M.C. (2015) ShakeMapNZ: Informing post-event decision making, Paper O-40 in: *New Dimensions in Earthquake Resilience: New Zealand Society for Earthquake Engineering Technical Conference*, 10-12 April, Rotorua, New Zealand

O'Rourke, M. and Deyoe E. (2004) Seismic Damage to Segmented Buried Pipe. *Earthquake Spectra,* 20(4):1167-1183

O'Rourke, T. D., Jeon, S.-s., Toprak, S., Cubrinovski, M., Hughes, M., Van-Ballegooy, S., et al. (2014) Earthquake Response of Underground Pipeline Networks in Christchurch, NZ. *Earthquake Spectra*, 30(1):183-204.

SCIRT (2013) Assessing assets to utilise remaining asset life and avoid repairing non-critical defects. Christchurch: SCIRT.

Rojahn, C. & Sharpe, R.L. (Principal Investigators) and expert panel (1985). Earthquake Damage Evaluation Data for California. *Report ATC-13*, Applied Technology Council, California.

Stirling, M.W., M.C. Gerstenberger, T. Goded and W. Ries (2015). Macroseismic intensity assessment for the M6.2 2011 Christchurch earthquake. *GNS Science Consultancy Report 2015/16*, 58 pp.

Worden, C.B., Gerstenberger, M.C., Rhoades, D.A. & Wald, D.J. (2012) Probabilistic Relationships between Ground Motion Parameters and Modified Mercalli Intensity in California. *Bulletin of the Seismological Society of America*, 102: 204-221. doi:10.1785/0120110156